

Space Station Zero-Propellant Maneuver Guidance Trajectories Compared To Eigenaxis

Nazareth Bedrossian, Sagar Bhatt

Abstract—The Zero-Propellant Maneuver (ZPM) guidance concept has been used on November 5, 2006, and March 3, 2007 to reorient the International Space Station (ISS) 90 deg and 180 deg respectively with Control Moment Gyroscopes (CMGs) without using any propellant. It will be shown that there are multiple ZPM trajectories that can perform the maneuver non-propulsively. Performing the same maneuver using an eigenaxis path would saturate the CMGs, requiring thrusters to regain attitude control. A condition is derived to explain why the CMGs saturate along the eigenaxis path. Flight results from the two ZPM demonstrations are presented.

I. INTRODUCTION

IN this paper, the Zero-Propellant Maneuver (ZPM) spacecraft guidance concept is described and compared to an eigenaxis approach. The ZPM is used to generate three different trajectories for a 90-deg rotation of the International Space Station (ISS). It is shown that maneuvering along the eigenaxis trajectory requires the use of propellant, whereas the ZPMs can be performed non-propulsively.

The ZPM concept is based on developing a special attitude trajectory that takes advantage of the nonlinear system dynamics to reduce or eliminate the “cost” of the maneuver. For example, an eigenaxis maneuver is kinematically the shortest path between two orientations. It is widely used due to its simplicity. However, to follow the eigenaxis, the inertial and disturbance dynamics must be overcome. By considering a kinematically longer path and increasing the time to perform the maneuver, path dependence of system dynamics can be exploited to achieve a “cost” lower than the equivalent eigenaxis maneuver. ZPMs can be used to perform transitions between pre-specified rotational states (i.e., attitude, rate, and momentum). Thus a ZPM can perform a large-angle attitude maneuver, damp rates, desaturate momentum, or some combination of all of these objectives.

Normally, ISS large-angle attitude maneuvers are performed using thrusters. For short-term attitude hold and maneuvers, a PID attitude hold controller with an eigenaxis maneuver logic is used to command the Control Moment

Gyroscopes (CMGs). However, the CMGs have limited torque and momentum capacity. Each of the four CMGs stores 4881 N-m-s (3600 ft-lbf-s) of angular momentum and can produce a torque up to 68 N-m (50 ft-lbf). Commanding a large-angle maneuver along the eigenaxis would cause the CMGs to rapidly reach their capacity limits, i.e., saturate. To regain control authority, thrusters would then have to be used. However, by commanding a ZPM trajectory, the CMGs can be maintained within their capacity limits as was flight demonstrated on November 5, 2006 and March 3, 2007 when the ISS was rotated 90 deg [1],[2] and 180 deg [3],[4] respectively.

This paper illustrates the ZPM guidance concept within the context of a specific ISS maneuver. After a description of the problem and operational implementation, three different trajectories are developed and their performance compared to an equivalent eigenaxis maneuver using high fidelity simulation. Finally, results from the two flight demonstrations are presented.

II. ZPM PROBLEM STATEMENT

A ZPM can be planned to minimize a user-specified “cost” by posing and solving an optimal control problem (OCP) for a specified maneuver time. The OCP in this context is to transition the spacecraft from an initial to a final rotational state while satisfying the system dynamics and maintaining the CMGs within their capability. The degrees of freedom are the commanded vehicle attitude and rate history with respect to the Local Vertical Local Horizontal (LVLH) reference frame.

The complete details of this OCP are described in [5]. In the following a brief outline of the problem is presented. For this paper, only time-invariant dynamics are considered, and the ISS system dynamics can be written as [6]

$$J\dot{\omega} = -\omega \times (J\omega + H_{CMG}) - \dot{H}_{CMG} + T_{gg}(\epsilon, \eta) + T_{aero}(\epsilon, \eta, x)$$

$$\dot{\epsilon} = \frac{1}{2}(\epsilon^x + \eta I)(\omega - \omega_{LVLH}(\epsilon, \eta))$$

$$\dot{\eta} = -\frac{1}{2}\epsilon^T(\omega - \omega_{LVLH}(\epsilon, \eta))$$

$$\epsilon^T \epsilon + \eta = 1$$

$$\dot{H}_{CMG} = u - \omega \times H_{CMG}$$

$$u = J(K_p \epsilon_{err} + K_D \dot{\epsilon}_{err})$$

where $\omega(t)$ is the inertial angular rate of the vehicle, J is the inertia matrix, $\epsilon(t)$ and $\eta(t)$ are Euler parameters representing

Manuscript received March 26, 2008.

Nazareth Bedrossian is Group Leader, Manned Space Systems at The Charles Stark Draper Laboratory, Inc., Houston TX 77058 (phone: 281-212-1104; e-mail: naz@draper.com).

Sagar Bhatt is Member of Technical Staff II, Manned Space Systems at The Charles Stark Draper Laboratory, Inc., Houston TX 77058 (phone: 281-212-1119; e-mail: sbhatt@draper.com).

attitude with respect to LVLH, $\mathcal{E}^x(t)$ is the skew-symmetric matrix for cross products, I is the identity matrix, $\omega_{LVLH}(t)$ is the LVLH rate, $x(t)$ is position along the orbit, $H_{CMG}(t)$ is total CMG momentum, $u(t)$ is the PD control torque, K_P and K_D are scalar proportional and derivative gains, and the errors between commanded and actual attitude and rate are $\mathcal{E}_{err}(t)$ and $\omega_{err}(t)$ respectively. All quantities are expressed in the ISS body-fixed reference frame. Also, the environmental disturbance torques are the gravity gradient torque T_{gg} , and the aerodynamic torque T_{aero} . Note that the environmental torques on the ISS are attitude (and position dependent), hence, the attitude trajectory influences the contribution of these terms.

The ZPM trajectory is then obtained by solving a particular OCP. One manifestation of the OCP that captures the general objectives mentioned above for a rotational maneuver is given by

$$\begin{aligned} \min & \int_{t_0}^{t_f} u^T(t)u(t) dt \\ \text{s.t.} & \\ & \dot{\omega}(t) = J^{-1} \left[-\omega(t) \times (J\omega(t) + H_{CMG}(t)) - \dot{H}_{CMG}(t) + T_{gg}(\mathcal{E}, \eta) + T_{aero}(\mathcal{E}, \eta, x) \right] \\ & \dot{\mathcal{E}}(t) = \frac{1}{2} (\mathcal{E}^x(t) + \eta(t)I) (\omega(t) - \omega_{LVLH}(\mathcal{E}, \eta)) \\ & \dot{\eta}(t) = -\frac{1}{2} \mathcal{E}^T(t) (\omega(t) - \omega_{LVLH}(\mathcal{E}, \eta)) \\ & \dot{H}_{CMG}(t) = u(t) - \omega(t) \times H_{CMG}(t) \\ & u(t) = J(K_P \mathcal{E}_{err}(t) + K_D \omega_{err}(t)) \\ & \text{Path Constraints} \\ & \mathcal{E}^T(t)\mathcal{E}(t) + \eta(t) = 1 \quad \forall t \in [t_0, t_f] \\ & H_{CMG}^T(t)H_{CMG}(t) \leq H_{\max} \quad \forall t \in [t_0, t_f] \\ & \dot{H}_{CMG}^T(t)\dot{H}_{CMG}(t) \leq \dot{H}_{\max} \quad \forall t \in [t_0, t_f] \\ & \text{Boundary Conditions} \\ & \mathcal{E}(t_0) = \mathcal{E}_0, \eta(t_0) = \eta_0, \omega(t_0) = \omega_0, H_{CMG}(t_0) = H_0 \\ & \mathcal{E}(t_f) = \mathcal{E}_f, \eta(t_f) = \eta_f, \omega(t_f) = \omega_f, H_{CMG}(t_f) = H_f \end{aligned}$$

Recent advances in pseudospectral (PS) methods [7],[8] have allowed for the efficient and rapid solution of optimal control problems governed by arbitrary nonlinear dynamical systems. For this reason, PS methods were used to solve the ZPM optimal control problem using the software package DIDO [9], which implements the Legendre PS method.

III. OPERATIONAL IMPLEMENTATION

To implement the ZPM, the ground-developed trajectory commands are time-tagged with the Greenwich Mean Time (GMT) for uplink to the Command and Control computer (C&C MDM) before maneuver execution begins. As a result, the ZPM commands are hardwired to start at the specified GMT times only. Because the C&C MDM command buffer is limited to 200 slots, the non-propulsive maneuver is allocated 160 slots and is composed of 80 command pairs (attitude and rate). Since the ISS attitude hold controller uses an eigenaxis maneuver logic, the rate command is a scalar maneuver rate required to transition from one attitude

command to the next in the specified time. Since the trajectory is defined in terms of commands to the PD controller, no flight software modifications are required for onboard implementation.

IV. COMPARISON OF 90-DEG ISS ROTATION TRAJECTORIES

In this section, three ZPM trajectories are compared to an eigenaxis trajectory for the ISS Stage 12A maneuver from +X-axis in Velocity Vector (+XVV) to +Y-axis in Velocity Vector (+YVV) flight attitude that was performed on November 5, 2006. To discover these different solutions to the OCP, various initial guesses were used to seed the optimization. The initial and final attitude targets with respect to LVLH were $[13 \ -9 \ 2]$ deg and $[-90 \ -8 \ -2]$ deg (YPR order and sequence) respectively. The initial and final CMG momentum targets were $[1356 \ -678 \ -5694]$ N-m-s and $[-12 \ -4823 \ -183]$ N-m-s respectively. The maneuver duration was chosen to be two hours.

Fig. 1 to Fig. 3 show the different ZPM trajectories as well as the eigenaxis trajectory for the same maneuver time (attitude with respect to LVLH in Yaw, Pitch, Roll sequence). All trajectories were verified in the high-fidelity Space Station Multi-Rigid Body Simulation (SSMRBS) [10]. The ‘‘Near-Eigenaxis’’ ZPM is similar to the eigenaxis and is close to the trajectory used for the November 5, 2006 ISS flight demonstration. The ‘‘Large-Roll’’ ZPM has a large attitude excursion from the eigenaxis path in roll, whereas the ‘‘Large-Yaw’’ ZPM performs the 90-deg yaw maneuver by rotating 270 deg in the opposite direction. The total angular distance traveled, the cumulative eigenangle, during each maneuver is shown in Fig. 4. The corresponding maneuver rate magnitudes are shown in Fig. 5. Note that for the eigenaxis, the maneuver rate is constant, while for ZPM it is not.

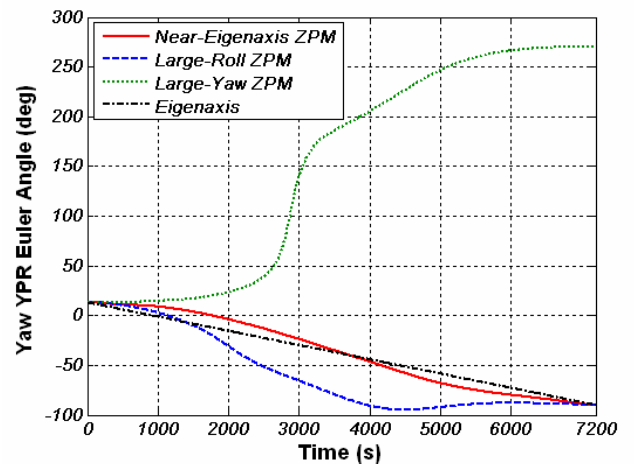


Fig. 1. Yaw angle for ZPM and Eigenaxis trajectories

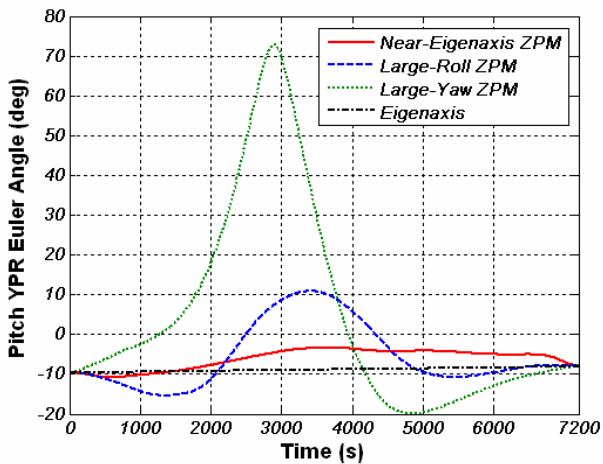


Fig. 2. Pitch angle for ZPM and Eigenaxis trajectories

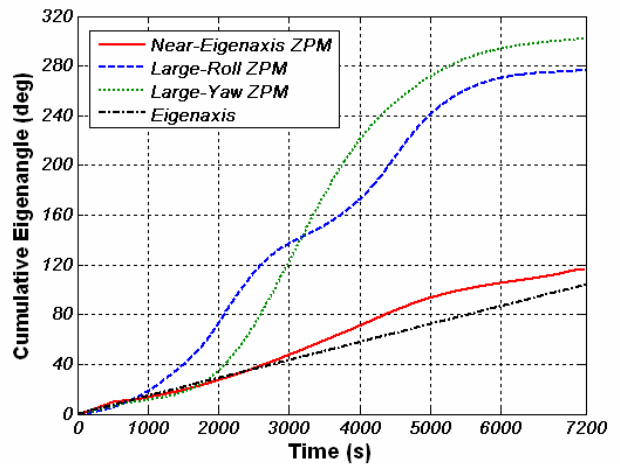


Fig. 4. Cumulative eigenangle for ZPM and Eigenaxis trajectories

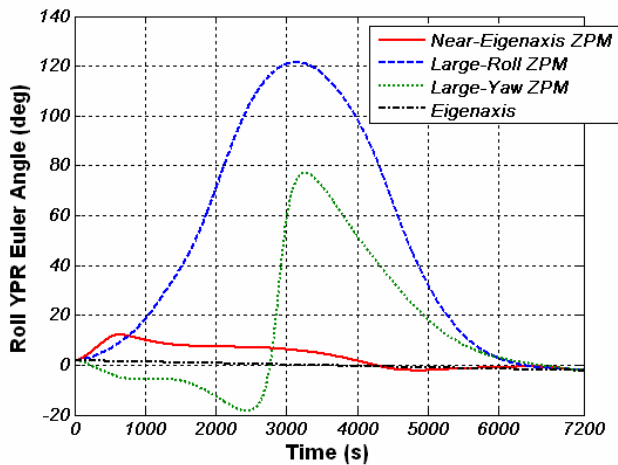


Fig. 3. Roll angle for ZPM and Eigenaxis trajectories

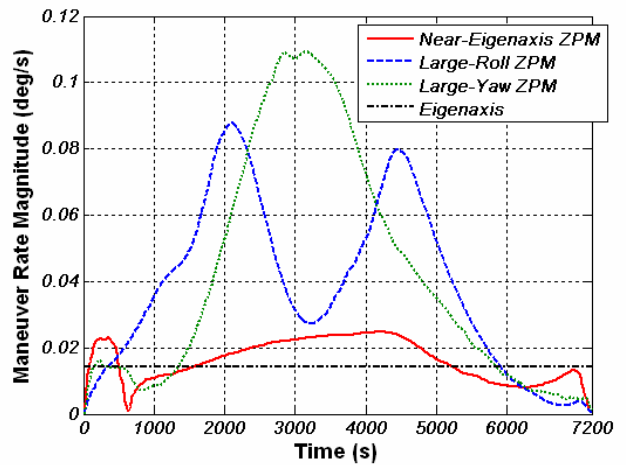


Fig. 5. Maneuver rate magnitude for ZPM and Eigenaxis trajectories

Following these distinct maneuver trajectories yields differences in maneuver cost and performance. The percentage of momentum capacity used is given in Fig. 6. For the eigenaxis trajectory, the CMGs saturate, resulting in loss of attitude control (not shown in the plots in Fig. 1-4). Thus the final attitude cannot be reached by following the eigenaxis without firing thrusters. Surprisingly, the trajectory with the lowest peak momentum is the “Large-Yaw” ZPM. In fact, both the “Large-Yaw” and “Large-Roll” trajectories have more momentum margin than the “Near-Eigenaxis” or eigenaxis trajectories despite traversing larger angular distances. However, the “Near-Eigenaxis” trajectory was selected by NASA for the flight demonstration since it was close enough to the nominal eigenaxis path as to not require additional thermal analysis.

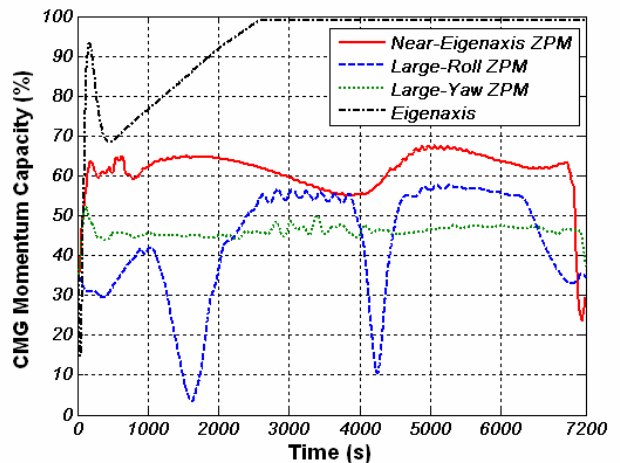


Fig. 6. CMG momentum capacity for ZPM and Eigenaxis trajectories

V. DIFFERENCE BETWEEN ZPM AND EIGENAXIS

The difference in performance between the ZPM and eigenaxis trajectories can be explained by the effort required

to overcome the system dynamics. To follow an eigenaxis path, the controller must negate the environmental dynamics with the CMG torque, which eventually leads to CMG saturation. In fact, for an eigenaxis rotation, the vehicle angular acceleration magnitude must remain constant:

$$\|\dot{\omega}\| = \|J^{-1}[-\omega \times (J\omega + H_{CMG}) - \dot{H}_{CMG} + T_{gg} + T_{aero}]\| = const.$$

To derive this claim, the following notation will be used. For a vector $z(t)$, let \dot{z} and z' be the derivatives of z with respect to a rotating reference frame and an inertial reference frame respectively. If ω is the angular rate of the rotating frame with respect to the inertial frame, then [6]

$$z' = \dot{z} + \omega \times z. \quad (1)$$

Therefore, for the ISS rate (measured in the body frame)

$$\omega' = \dot{\omega} + \omega \times \omega = \dot{\omega}.$$

Expressing the rate in the LVLH frame does not change its magnitude [6], so that

$$\|\dot{\omega}\| = \|\omega'\| = \|\omega'^L\|$$

where the superscript L denotes the quantity is expressed in the LVLH frame. Reapplying (1) with LVLH as the rotating frame gives

$$\|\omega'^L\| = \|\dot{\omega}^L + \omega_{LVLH}^L \times \omega^L\|. \quad (2)$$

The ISS rate is the sum of the LVLH rate and maneuver rate (i.e., the body rate relative to LVLH):

$$\omega^L = \omega_{LVLH}^L + \omega_{mvr}^L. \quad (3)$$

Since the orbital rate ω_{orb} is constant for a circular orbit and

$$\omega_{LVLH}^L = \begin{bmatrix} 0 \\ -\omega_{orb} \\ 0 \end{bmatrix},$$

the LVLH rate is constant in the LVLH frame:

$$\dot{\omega}_{LVLH}^L = 0. \quad (4)$$

Moreover, for an eigenaxis maneuver the controller maintains a single fixed maneuver rate. The maneuver rate is the product of the unit eigenaxis vector and the total eigenangle divided by the maneuver time. The orientation of the eigenaxis relative to both the LVLH and body frames remains unchanged throughout an eigenaxis maneuver [11], and so

$$\dot{\omega}_{mvr}^L = 0. \quad (5)$$

Thus (3)-(5) imply that during an eigenaxis maneuver the ISS rate measured in the LVLH frame does not change:

$$\dot{\omega}^L = 0. \quad (6)$$

Substituting (6) and (3) into (2) gives

$$\begin{aligned} \|\omega'^L\| &= \|\dot{\omega}^L + \omega_{LVLH}^L \times \omega^L\| \\ &= \|\omega_{LVLH}^L \times \omega^L\| \\ &= \|\omega_{LVLH}^L \times (\omega_{LVLH}^L + \omega_{mvr}^L)\| \\ &= \|\omega_{LVLH}^L \times \omega_{mvr}^L\| = const. \end{aligned}$$

Therefore, the following must hold along the eigenaxis trajectory:

$$\|\dot{\omega}\| = const.$$

For the eigenaxis maneuver for November 5, this constant

acceleration magnitude should be $1.7 \times 10^{-5} \text{ deg/s}^2$.

The acceleration magnitude for the eigenaxis trajectory is compared to the ZPM in Fig. 7. After an initial startup transient, the eigenaxis acceleration magnitude settles at the predicted constant value until the CMGs saturate (at about 2600 s into the maneuver). Because the maneuver rate is variable for the ZPM, no such acceleration constraint is present and the ZPM can use the disturbance torques to its advantage. As a result, a ZPM enables non-propulsive control by maintaining the CMGs within capacity, as demonstrated in the flight tests, presented next.

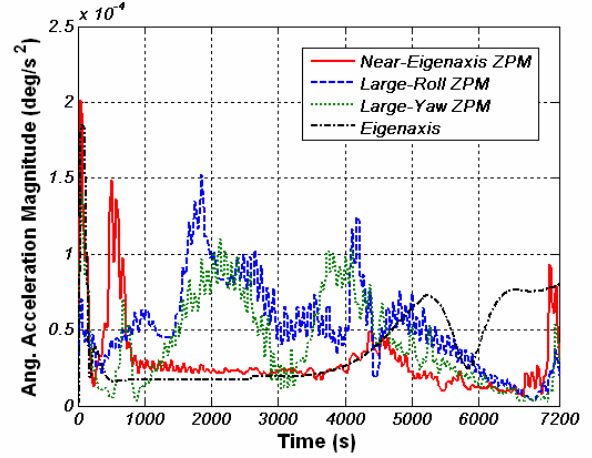


Fig. 7. Angular acceleration magnitude for ZPM and Eigenaxis trajectories

VI. FLIGHT RESULTS

For the first ZPM flight demonstration [1],[2],[5] on November 5, 2006, a trajectory similar to the “Near-Eigenaxis” ZPM was flown to perform a 90-deg yaw rotation. The ISS flight telemetry screenshots for percent of CMG momentum capacity used and commanded versus actual attitude are shown in Fig. 9 and Fig. 8. There were two periods when the ISS state telemetry signal was lost. Coincidentally, the loss of signal periods occurred at the most dramatic times, namely at the beginning and end of the maneuver when the momentum was rapidly changing. The maneuver was completed in 2 hours with a new command pair (attitude and maneuver rate magnitude) issued every 90 s. The peak momentum magnitude remained below 70% of CMG capacity. The transition to long-term attitude control was successful.

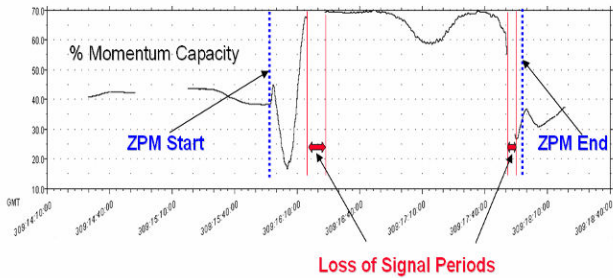


Fig. 8. Flight telemetry momentum capacity for 90-deg ZPM on November 5, 2006.

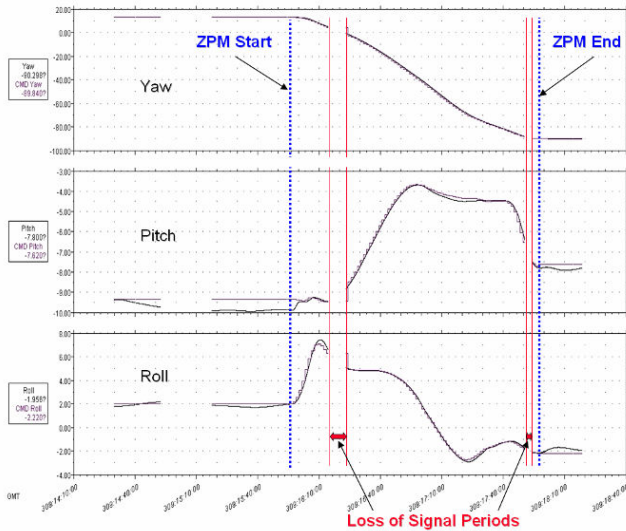


Fig. 9. Flight telemetry commanded and actual attitude for 90-deg ZPM on November 5, 2006.

Following the first ZPM flight test, a 180-deg ISS ZPM [3],[4] was performed on March 3, 2007. The maneuver from +XVV to -XVV was completed in 2 hours and 47 minutes with commands issued every 125 s. The flight telemetry momentum and attitude are shown in Fig. 11 and Fig. 10 respectively. The peak momentum reached 76% of CMG capacity. The propellant savings were significant as the identical 180-deg reorientation performed with thrusters on January 2, 2007 consumed 50.8 kg of propellant at an estimated cost of \$1,100,000.

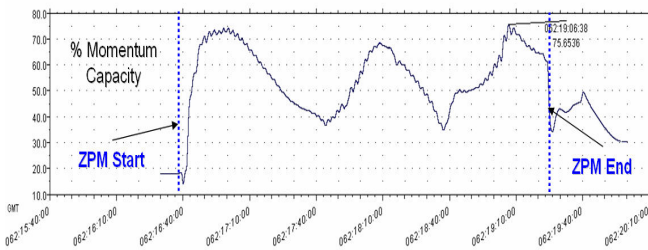


Fig. 10. Flight telemetry momentum capacity for 180-deg ZPM on March 3, 2007.

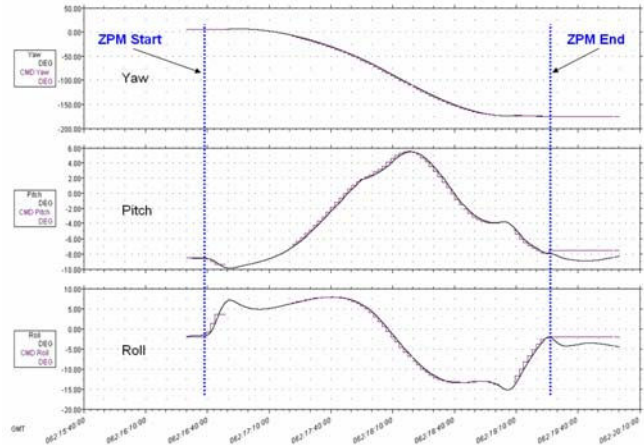


Fig. 11. Flight telemetry commanded and actual attitude for 180-deg ZPM on March 3, 2007.

VII. CONCLUSION

Multiple Zero-Propellant Maneuver (ZPM) guidance trajectories were developed for a specific International Space Station (ISS) 90-degree attitude maneuver. It was shown that maneuvering along the eigenaxis required the use of propellant whereas the ZPM maneuvers were performed non-propulsively, thereby significantly reducing spacecraft propellant requirements. With ZPM, a new class of performance previously thought impossible can be achieved, including large-angle maneuvers, rate damping [12], momentum dumping [13], and control with saturated CMGs [12]. Moreover, ZPM is a flight proven technology. On November 5, 2006 and March 3, 2007, ZPMs were used to non-propulsively rotate the ISS 90 deg and 180 deg respectively.

REFERENCES

- [1] Bedrossian, N., Bhatt, S., Lammers, M., Nguyen, L., and Zhang, Y., "First Ever Flight Demonstration of Zero Propellant Attitude Control Concept", *2007 AIAA GN&C Conference*, 20-23 August 2007, Hilton Head, SC, AIAA 2007-6734.
- [2] YouTube website, "First-Ever Space Station Zero-Prop Maneuver (ZPM)," 19 November, 2007, [Online]. Available: http://www.youtube.com/watch?v=Mlp27Ea9_2I.
- [3] Bedrossian, N., Bhatt, S., Lammers, M., Nguyen, L., "Zero Propellant Attitude Control Flight Results for 180° ISS Rotation", *2007 International Symposium on Space Flight Dynamics*, 24-28 September 2007, Annapolis, MD, NASA/CP-2007-214158.
- [4] YouTube website, "180deg Space Station Zero-Prop Maneuver (ZPM)," 19 November, 2007, [Online]. Available: <http://www.youtube.com/watch?v=kyPNzVzy36M>.
- [5] Bhatt, S., "Optimal Reorientation of Spacecraft Using Only Control Moment Gyroscopes," Master's thesis, Dept. of Computational and Applied Mathematics, Rice University, 2007. Available: <http://www.keck.caam.rice.edu/caam/trs/2007/TR07-08.pdf>.
- [6] Hughes, P. C., *Spacecraft Attitude Dynamics*, John Wiley and Sons, New York, 1986.
- [7] Ross, I. M., and Fahroo, F., "Legendre Pseudospectral Approximation of Optimal Control Problems," *Lecture Notes in Control and Information Sciences*, Vol. 295, Springer-Verlag, New York, 2003.
- [8] Ross, I. M. and Fahroo, F., "Pseudospectral Knotting Methods for Solving Optimal Control Problems," *Journal of Guidance, Control and Dynamics*, Vol. 27, No. 3, pp.397-405, 2004.

- [9] Ross, I. M., "A Beginner's Guide to DIDO: A MATLAB Application Package for Solving Optimal Control Problems," Elissar Inc., Monterey, CA, October 2007.
- [10] Sebelius, K., "Version Baseline 3.7 Release of Space Station Multi-Rigid Body Simulation," ESCG-4370-06-OGNC-MEMO-0025, 30 November, 2005.
- [11] Wie, B., *Space Vehicle Dynamics and Control*. AIAA Education Series, Ohio, 1998.
- [12] Bedrossian, N., Bhatt, S., Alaniz, A., McCants, E., Nguyen, L., Chamitoff, G., "ISS Contingency Attitude Control Recovery Method for Loss of Automatic Thruster Control," *31st AAS Guidance and Control Conference*, 1-6 February 2008, Breckenridge, CO, AAS 08-001.
- [13] Pietz, J., Bedrossian, N., "Momentum Dumping Using Only CMGs," *2003 AIAA GN&C Conference*, 11-13 August 2003, Austin, TX.